Received: 3 January 2023 | Accepted: 10 March 2023

DOI: 10.1111/bcpt.13860

ORIGINAL ARTICLE

BCPT Basic & Clinical Pharmacology & Toxicology

Monitoring paxillin in astrocytes reveals the significance of the adhesion G protein coupled receptor VLGR1/ADGRV1 for focal adhesion assembly

Baran E. Güler | **Joshua Linnert** | **Uwe Wolfrum**

Institute of Molecular Physiology, Molecular Cell Biology, Johannes Gutenberg University Mainz, Mainz, Germany

Correspondence
Uwe Wolfrum, Institute of Molecular Physiology, Molecular Cell Biology, Johannes Gutenberg University Mainz, Hanns-Dieter-Hüsch-Weg 17, 55128 Mainz, Germany.
Email: wolfrum@uni-mainz.de

Funding information
Deutsche Forschungsgemeinschaft DFG FOR 2149, project number 246212759 (UW), and The Foundation Fighting Blindness (FFB) PPA-0717-0719-RAD (UW), inneruniversitäre Forschungsförderung ("Stufe I") of the Johannes Gutenberg University Mainz (UW).

Abstract

VLGR1/ADGRV1 (very large G protein-coupled receptor-1) is the largest adhesion G protein-coupled receptor (aGPCR). Mutations in *VLGR1/ADGRV1* are associated with human Usher syndrome, the most common form of deaf-blindness, and also with epilepsy in humans and mice. VLGR1 is expressed almost ubiquitously but is mainly found in the CNS and in the sensory cells of the eye and inner ear. Little is known about the pathogenesis of the diseases related to VLGR1. We previously identified VLGR1 as a vital component of focal adhesions (FAs) serving as a metabotropic mechanoreceptor controls cell spreading and migration. FAs are highly dynamic and turnover in response to internal and external signals. Here, we aimed to elucidate how VLGR1 participates in FA turnover. Nocodazole washouts and live cell imaging of paxillin-DsRed2 consistently showed that FA disassembly was not altered, but de novo assembly of FA was significantly delayed in *Vlgr1*-deficient astrocytes, indicating that VLGR1 is enrolled in FA assembly. In FRAP experiments, recovery rates were significantly reduced in *Vlgr1*-deficient FAs, indicating reduced turnover kinetics in VLGR1-deficient FAs. We showed that VLGR1 regulates cell migration by controlling the FA turnover during their assembly and expect novel insights into pathomechanisms related to pathogenic dysfunctions of VLGR1.

KEYWORDS
aGPCR, cell migration, epilepsy, focal adhesions, G protein-coupled receptors, mechanoreception, Usher syndrome

1 | INTRODUCTION

VLGR1 (very large G protein-coupled receptor-1), also known as GPR98 and MASS1 and recently renamed to ADGRV1,[1] belongs together with other 33 members to the G protein-coupled receptor (GPCR) family of adhesion G protein-coupled receptors (aGPCRs).[2] Among various VLGR1 isoforms, full-length VLGR1b is the largest G-protein coupled receptor in the human body with a molecular weight of ~700 kDa.[3] VLGR1/ADGRV1 is a

classical aGPCR characterized by a large extracellular domain (ECD), which contains 35 putative Ca^{2+}-binding calx-ß motifs, pentaxin/laminin G-like repeats (LAMG/PTX), epilepsy-associated/epitemptin-like domain (EPTP/EAR), the 7-transmembrane domain (7TM), and the relatively short cytoplasmic intracellular domain (ICD) with a class I PDZ domain-binding motif (PBM) at the very C terminal end (Figure 1). Autocleavage at the auto proteolysis site (GPS) localized within GAIN (GPCR auto-proteolysis-inducing) domain leads to a C-terminal fragment (CTF) and an N-terminal fragment (NTF), which can function independently.[4,5] There is growing evidence that after autocleavage, the short so-called "Stachel" sequence in the very N-terminal end of CTF is exposed and can act as a tethered agonist activating aGPCRs.[6,7] We have recently found an 11 amino acid sequence as the "Stachel" peptide of VLGR1.[5] We also found evidence that this activation induces a switch from Gs- to Gi-mediated signalling of VLGR1.

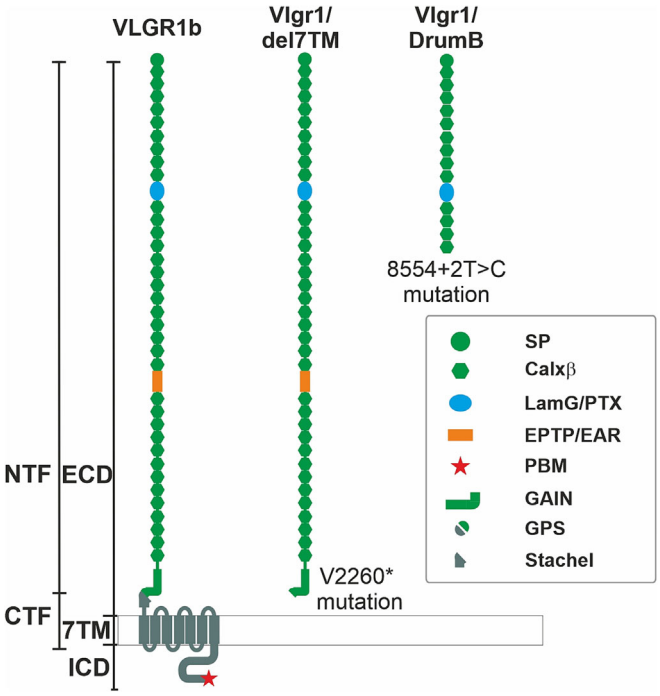

FIGURE 1 Domain structure of VLGR1/ADGRV1 and mutations in *Vlgr1* mouse models. VLGR1 is composed of an extremely long extracellular domain (ECD), 7-serpentine transmembrane domain (TM), and a relatively short intracellular domain (ICD) with a characteristic PDZ binding motif (PBM). The ECD includes a signal peptide (SP), 35 Ca^{2+} binding calcium exchanger β motifs (Calx-β), pentaxin/laminin G-like repeats (LAMG/PTX), an epilepsy-associated/Epitemptin-like domain (EPTP/EAR), a GPCR autoproteolysis-inducing domain (GAIN), which includes the G-protein-coupled receptor proteolytic site (GPS). Autoproteolytic cleavage at the GPS can result N-terminal fragment (NTF) and the C-terminal fragment (CTF) and the exposer of the Stachel sequence at the very N-terminal end of the CTF which can act as tethered agonist. In Vlgr1/del7TM mice V2260* nonsense mutation introduces a STOP codon which leads to the deletion of 7TM and ICD domains of *Vlgr1* and translation product is only ECD. In the Vlgr1/DrumB mice, the 8554+2t>c mutation leads to a STOP codon in intron 37–38. Translation product is a relatively short truncated protein, which includes only 13 CalXbeta domains and the LAMG domain.

The expression of VLGR1 is almost ubiquitously but highly concentrated in the central nervous system (CNS), especially during development and the sensory cells of the eye and inner ear[3] (Protein Atlas: https://www.proteinatlas.org/). Mutations in the *VLGR1/ADGRV1* gene cause human Usher syndrome 2C (USH), a subtype of the most common combined hereditary deaf-blindness disease.[8,9] In addition, it has been found that different mutations in mouse models for *Vlgr1/Adgrv1* are associated with audiogenic epilepsy.[3] However, over the last years, there is also growing evidence that mutations in *VLGR1/ADGRV1* also can cause different forms of epilepsy in humans.[10,11] Concrete knowledge of VLGR1's molecular function and signalling is necessary for gaining insights into the pathomechanisms and the elucidation of potential targets for therapies of diseases related to VLGR1.

In cochlear hair cells of the inner ear and the retinal photoreceptor cells, VLGR1 is essential for the formation of fibrous links spanning between neighbouring membranes.[12,13] While it is thought that the absence of these membrane attachment fibres underlie the sensory neuronal degeneration in the eye and ear causing USH, the processes leading to epilepsy due to defects in VLGR1 are completely unclear to date.

Applying affinity proteomics, we have previously identified numerous proteins related to focal adhesions (FAs) as potential interaction partners of VLGR1.[4,5,14] FAs are large supramolecular assemblies at contact sites of the cell membrane with the extracellular matrix.[15] The dynamic turnover, controlled assembly, and disassembly of FAs play a key role in cell spreading and migration. In this regard, FAs are essential for sensing and integrating intracellular signals as well as signals from the environment that control cell migration.[16] We have previously shown that VLGR1 is part of the multiprotein complex of FAs[5] and essential for their proper size and abundance in the cell.[14,17] More importantly, we have also demonstrated that VLGR1 in FAs functions as a metabotropic mechanoreceptor and controls cell spreading and migration.[14] However, it remained unknown how VLGR1 participates in the control of the dynamics of FAs during cell migration.

In the present study, we aimed to elucidate how VLGR1 controls the FA turnover during cell migration by applying nocodazole washout assays and live-cell imaging fluorescence recovery after photobleaching (FRAP) experiments. Our data conclusively demonstrate

that VLGR1 regulates cell migration by controlling the assembly of FA. From our findings, we also expect novel insights into pathomechanisms related to molecular and cellular dysfunction of VLGR1 in the developing and mature CNS.

2 | MATERIAL AND METHODS

2.1 | Animals

All animal experiments were performed per the guidelines of the Association for Research in Vision and Ophthalmology. Vlgr1/del7TM mice carry a premature STOP codon at exon 82 of *Vlgr1*, namely, the V2250* nonsense mutation of *Vlgr1*, which leads to the deletion of the entire 7TM domain and only the expression of the extracellular domain.[18] Drum B mice carry c.8554+2t>c mutation in exon 37 of Vlgr1 which results in an early STOP codon in intron 37–38 and if no splicing event occurs, the translation product only contains the first 13 CalXbeta domains and the LamG/PTX domain.[19] Both *Vlgr1*-deficient mouse lines are bred on a C57BL/6 background.

2.2 | Isolation of primary astrocytes from murine brains

Astrocytes were isolated from brains of postnatal day 0 (PN0) female and male sibling mouse pups as previously described.[17] Briefly, P0 mouse pups were dissected and cortexes were enzymatically and mechanically disassociated. Single-cell suspensions were seeded on PLL-coated T75 flasks and cultured in DMEM/10% FBS/2% penicillin/streptomycin (Thermo Fisher Scientific) for 7 to 10 days. Upon confluence, oligodendrocytes and neurons were removed by shaking the flasks. To isolate primary astrocytes from microglia cells, cultures were trypsinized and cell suspensions were seeded on successive dishes. While microglia cells attached to the surface of dishes, astrocytes could be collected from the supernatant. Isolated primary astrocytes were cultured additional 7–10 days in a complete growth medium.

2.3 | Cell culture

Primary astrocytes isolated from postnatal stage day 0 (PN0) mice were cultured in DMEM/10% FBS/20mM l-glutamine 1% penicillin/streptomycin. Half of the culture medium was changed on days 1, 2, 7, and 14 after the first isolation. Only passage 1 of astrocyte cultures was used for the experiments to maintain experimental consistency.

2.4 | Antibodies, fluorescent tools, and DNA constructs

We used the following primary antibodies: a rabbit monoclonal (ab32115) (Abcam) and a mouse monoclonal (BD Transduction Laboratories, 610 052) antibody against paxillin, and a rabbit polyclonal antibody against the C terminal of murine Adgrv1/Vlgr1.[13] Secondary antibodies conjugated to Alexa488, and Alexa647 was purchased from Molecular Probes (Life Technologies) or Rockland Immunochemicals. DNA counterstained with 4′,6-diamidino-2-phenylindole (DAPI, Merck). The Paxillin-DsRed2 plasmid was kindly provided by Drs. Rudolf E. Leube and Rick Hortwitz.[20]

2.5 | Immunocytochemistry

Primary astrocytes were fixed with 2% paraformaldehyde for 10 min. After fixations, specimens were washed twice, permeabilized with 0.2% Triton-X in PBS (Carl Roth GmbH) for 15 min, and quenched with 50-mM NH_4Cl for 5 min. Before primary antibody treatment, cells were blocked with 0.1% ovalbumin and 0.5% fish gelatin in PBS. Primary antibodies were incubated at 4°C overnight. After removing unbound antibodies by PBS washing, secondary antibodies were incubated at room temperature for 1 h, and an additional wash with H_2O, and coverslips were mounted with Mowiol 4.88 (Hoechst).

2.6 | Nocodazole-induced FA disassembly assay

FA disassembly assay was performed as described previously with slight modifications[21]; 1.5×10^5 primary murine brain astrocytes were seeded onto fibronectin-coated coverslips. After 48 h of culturing, cells were treated with 10-μM nocodazole (AppliChem GmbH) in 0.3% DMSO for 4 h in a serum-free medium. Subsequently, NDZ was washed out three times with 1× PBS, and upon washout, fresh complete growth medium was added. Coverslips were removed from the medium at time points 0, 15, 30, 45, 60, and 120 min, and cells were fixed and stained for FAs during microtubule polymerization.

2.7 | Morphometric analysis of FAs

Paxillin FA marker was used for FAs number analysis. The number of FAs was quantified as described in Güler

et al.[17] using Fiji image analysis software (https://fiji.sc). Briefly, images were converted to 8-bit images and the background was normalized with FFT Bandpass filter. Filtered images are thresholded and converted to binary images. FA numbers are analysed with the "analyse particles" built-in function. The minimum FA size is defined as 40 pixels. Finally, the total number of FAs was divided by cell area to determine FA numbers in μm^2.

2.8 | FA turnover analysis

For live-cell imaging analysis of FA turnover, ~35 000 cells were seeded on a 5 μg/ml fibronectin-coated μ-Slide 4 Well chamber (Ibidi) 72 h before imaging. The day after seeding, cells were transfected with Paxillin-DsRed2 construct with GeneJuice® transfection reagent (Merck Millipore). Transfections were performed according to the manufacturer's instructions. Cells were incubated for an additional 48 hours at 37°C with 5% CO2 in the incubator. Before starting live-cell imaging, the temperature of the incubation chamber was brought to 37°C with 5% CO_2 supply. Imaging was performed with Nikon Eclipse Ti2-E/Yokogawa CSU-W1 Spinning disk microscope using 100×/oil objectives. Live-cell movies were acquired at 1 frame/5 min with 10 z-stacks for a total 155 min. Images were analysed using Focal Adhesion Analysis Server (FAAS) (https://faas.bme.unc.edu/).[22] Maximum projections were applied to the image series and converted to 8-bit before uploading to the server. Adhesion size was defined as 10 pixels and the FA phase length was determined as five continuous image sets in the entire image analysis to provide experimental consistency. FAAS automatically detect and calculate FA assembly/disassembly rates based on changes in intensities during imaging. Life cell imaging also allowed us to determine the lifetime of FAs: The time span that encompasses the entire FA turnover cycle, that is, the time between the first appearance of an individual FA, the assembly, and the subsequent disassembly, until the disappearance of a FA.

2.9 | FRAP in primary astrocytes

For FRAP analysis, we used Paxillin-DsRed2 expressed wild type and *Vlgr1*-deficient astrocytes. Before photobleaching cells were imaged every 20 s for total 120 s to define basal bleaching rates. After 120 s of imaging, randomly selected FAs from the periphery of the cells were photobleached with 561-nm laser set to 100% power. To quantify FA kinetics, raw intensity values photobleached area (ROI1), whole cell (ROI2), and background area (ROI3) were measured with Fiji image analysis software. Intensity values were uploaded to the easyFRAP online tool (https://easyfrap.vmnet.upatras.gr/).[23] Post-bleached intensity values were normalized by subtracting pre-bleach values for bleach correction. Full-scale normalization was applied for FRAP fluorescence intensity curves and T-half time and mobile fractions were calculated with double curve fitting function. Only p values less than 0.05 are taken under consideration for quantifications. Samples were analysed with a Nikon Eclipse Ti2-E/Yokogawa CSU-W1 Spinning disk microscope using 63×/water objectives.

The study was conducted in accordance with the Basic & Clinical Pharmacology & Toxicology policy for experimental and clinical studies.[24]

3 | RESULTS

3.1 | Nocodazole washout assays revealed enrolment of VLGR1 in the assembly of FAs

We have previously shown that VLGR1 is vital for FAs affecting the size and length of FAs as well as the velocities of cell spreading and migration.[14] However, it has remained unclear/open whether VLGR1 controls migration capacity and turnover of FA during the assembly or the disassembly of FAs. We performed washout assays with the microtubule depolymerization drug nocodazole (NDZ), previously introduced to monitor the disassembly of FAs[21] (Figure 2A). We treated primary astrocytes derived from the brains of *Vlgr1*-deficient Vlgr1/DrumB mutant mice or wild type (WT) mice with either DMSO or nocodazole (NDZ) (10 μM) in DMSO. Consistent with previous reports,[21,25,26] NDZ treatment induced microtubule depolymerization leading to cell-cycle synchronization and accumulation of FAs (Figure 2A,B). After replacing the NDZ medium by a fresh medium without NDZ (NDZ washout) a phase of rapid FA disassembly was introduced which rested for approximately 45 min (Figure 2A,B). Quantifying the number of FAs after the 4-h NDZ treatment and during the FA disassembly phase, we did not observe significant differences between WT and *Vlgr1*-deficient mice in the number of FAs (Figure 2C, time points 15 to 45 min).

After 45 min of NDZ washout, the FA disassembly phase was followed by a phase of de novo assembly of FAs, characterized by increasing numbers of FAs in the primer astrocytes of mouse lines (Figure 2A,B; time points 60 and 120 min after NDZ washout).[21] Quantifying the number of FAs during this FA de novo

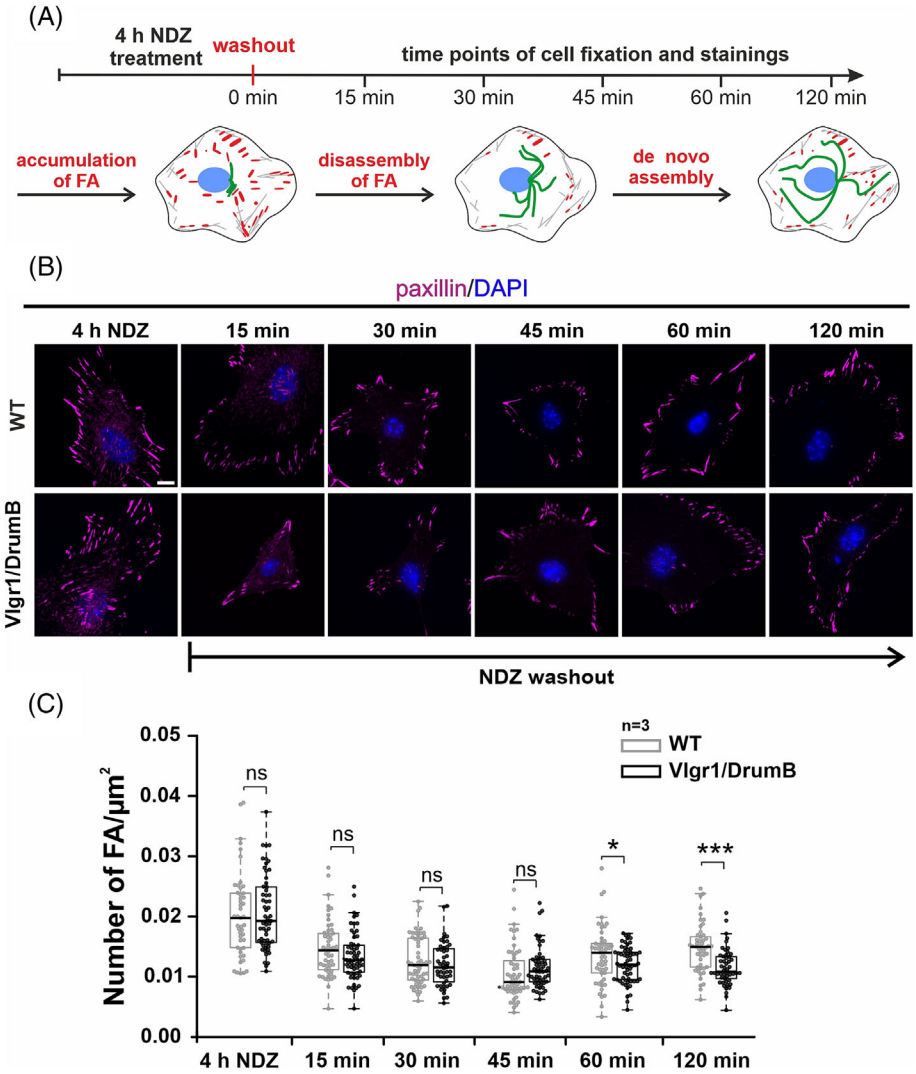

FIGURE 2 Analysis of focal adhesion (FA) turnover in primary astrocytes by nocodazole washout assays. (A) Scheme of nocodazole (NDZ) washout assay. Primary murine astrocytes were incubated with 10 uM NDZ in serum-free medium for 4 h to induce FA accumulation. Subsequent NDZ washout with complete growth medium induces FA disassembly (15–45 min), before de novo assembly starts at 60–120 min. (B) Immunostaining of the FA marker paxillin (magenta) and nuclear counterstaining of DAPI (blue) in primary astrocytes derived from wild type (WT) and *Vlgr1*-deficient Vlgr1/DrumB mouse hippocampi at different time points after NDZ washout. (C) Quantification of FA numbers after NDZ washout. In the FA disassembly phase (15–45 min after NCD washout), FA numbers steadily decreased in both WT and in *Vlgr1*-deficient Vlgr1/DrumB astrocytes without a significant difference. During the de novo assembly of FAs (60, 120 min), the number of FAs was significantly lower in *Vlgr1*-deficient Vlgr1/DrumB. $N = 47–58$ cells in WT astrocytes and 48–62 cells in Vlgr1/DrumB astrocytes per time-points were analysed in $n = 3$ independent experiments. Data are represented as mean ± SD. Statistical evaluation was performed using two-tailed Mann–Whitney *U* test, **p* % 0.05, ***p* % 0.01, ****p* % 0.001. Scale bars: 10 µm.

assembly phase revealed a significantly lower number of FAs in *Vlgr1*-deficient astrocytes when compared to WT astrocytes (Figure 2B,C). In contrast, we did not observe any changes in FA numbers in controls in which we only treated the astrocytes of both mouse lines with DMSO (Figure S1A,B). Taken together, the NDZ washout experiments showed that the absence of VLGR1 did not affect the disassembly of FAs but rather indicated a role of VLGR in the assembly of FAs.

3.2 | Live-cell imaging demonstrated that VLGR1 controls FA assembly in the living cell

Next, we analysed the FA turnover by live-cell imaging of primary astrocytes of WT and *Vlgr1*-deficient mice expressing the FA marker Paxillin-DsRed2.[17] Immunostaining of astrocytes demonstrated the co-localization of VLGR1 and Paxillin-DsRed2 confirming our previous results on VLGR1 and paxillin (Figure S2).[14]

For live-cell imaging, we recorded Paxillin-DsRed2-labelled FAs in *Vlgr1*-deficient primary astrocytes derived from Vlgr1/DrumB mice and WT astrocytes for 2 h in a spinning disc confocal microscope (Videos S1 and S2). Subsequently, we analysed and quantified the dynamics of Paxillin-DsRed2-FAs in these video tracks by applying the FAAS web tool (https://faas.bme.unc.edu)[22] (Figure 3). To eliminate putative background signals in FAAS analyses, FA sizes were defined minimum of 10 pixels and assembly/disassembly processes were

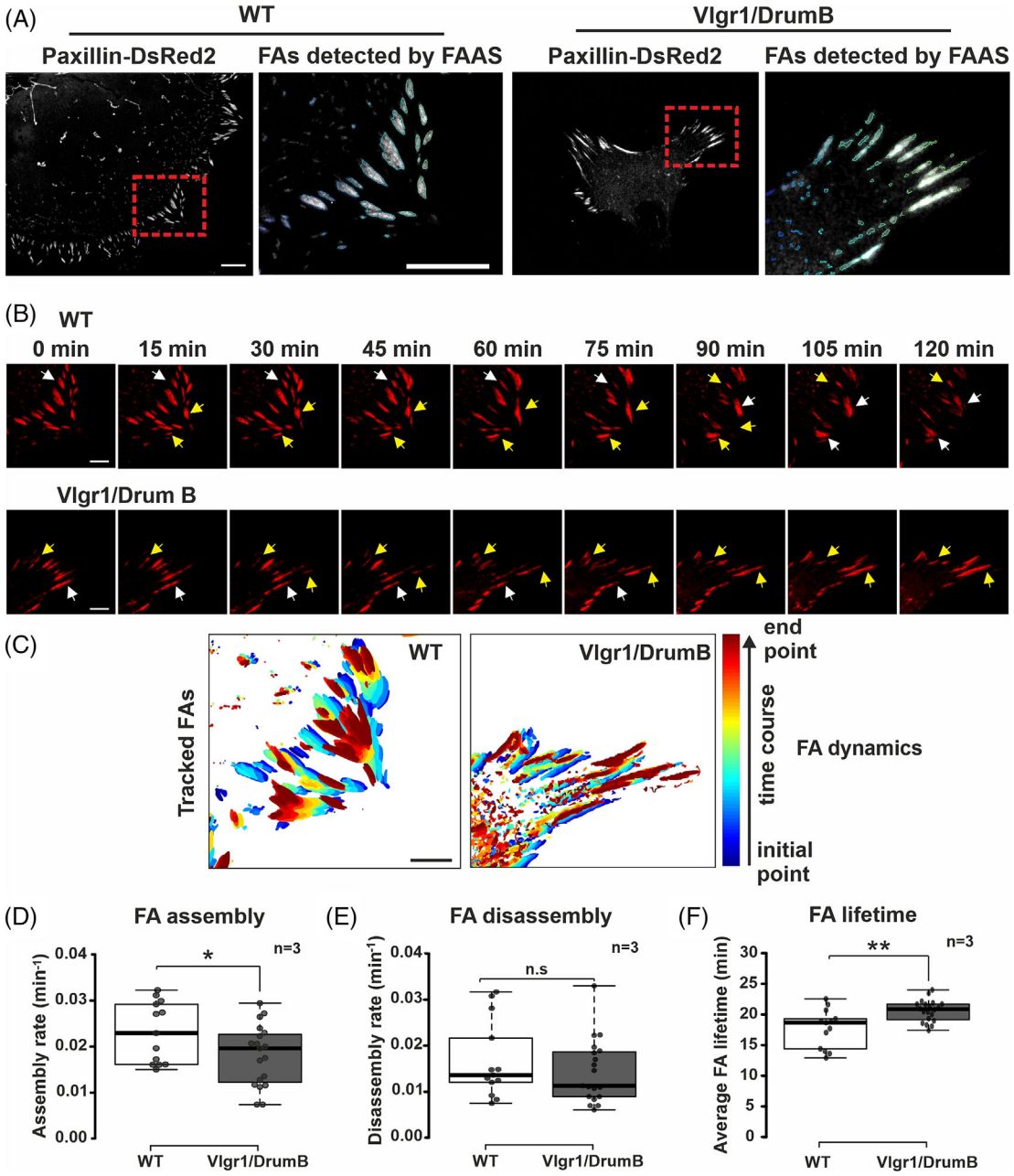

FIGURE 3 Live-cell imaging analysis of FAs turnover in primary astrocytes *Vlgr1*-deficient Vlgr1/DrumB mice. (A) Identification of FAs Paxillin-DsRed2 fluorescence image analysis by the Focal Adhesion Analysis Server (FAAS) (https://faas.bme.unc.edu) in wild type (WT) and *Vlgr1*-deficient Vlgr1/DrumB astrocytes expressing Paxillin-DsRed2. (B) Time-lapse image sequences of Paxillin-DsRed2 in FAs from WT and Vlgr1-deficient Vlgr1/DrumB astrocytes selected every 15 min from video traces recorded with a sequence of 5 min in a time course of 155 min. *Yellow arrow heads* point to assembling FAs and *white arrow heads* point to disassembling FAs. (C) Pseudo-coloured tracked FA images in WT and Vlgr1/DrumB astrocytes indicate initial and end points of assembly and disassembling FAs. Quantification of FA assembly rates (D), FA disassembly rates (E), and the average FA lifetime (F) in WT and Vlgr1/DrumB astrocytes. Cell numbers: $N = 13$ (WT), $N = 20$ (Vlgr1/DrumB) in $n = 3$ independent experiments. Data are represented as mean ± SD. Statistical evaluation was performed using two-tailed Student's t test, *p % 0.05, **p % 0.01, ***p % 0.001. Scale bars: 10 μm.

determined by using FAs, which appeared in five continuous image sets (Figure 3A). Following individual FAs (identified by FAAS) in time-lapse image sequences of Paxillin-DsRed2 in WT and Vlgr1/DrumB astrocytes, we observed that FAs undergo rapid assembly and disassembly in WT astrocytes, while the turnover of FAs was slower in Vlgr1/DrumB astrocytes (Figure 3B). The spatiotemporal dynamics in living astrocytes of WT and Vlgr1/DrumB were visualized by superposition of all FAs from microscopy image taken every 5 min during the entire time course of 155 min of colour for the set of FAs at each time point (Figure 3C).

Quantifications of all FAs in the analysed cells revealed that the assembly rate of FAs (Figure 3D) was significantly higher in WT astrocytes when compared to Vlgr1/DrumB astrocytes. In contrast, the disassembly rates did not significantly differ between both (Figure 3D). The lifetime of FAs (Figure 3F) was significantly longer in Vlgr1/DrumB astrocytes compared to WT astrocytes. To verify these results on FAs in Vlgr1/DrumB astrocytes, we also examined primary astrocytes derived from brains of Vlgr1/Del7TM mice (Figure S3), another *Vlgr1*-deficient mouse line.[18] Analogous live-cell imaging experiments showed, as in Vlgr1/DrumB astrocytes, no differences in the rate of FA disassembly but a significantly lower assembly rate of FAs in Vlgr1/Del7TM astrocytes compared with WT (Figure 3D,E; Figure S3C,D). In contrast to Vlgr1/DrumB, we did not observe differences in the life time of FAs in astrocytes of Vlgr1/del7TM (Figure S3E).

Taken together, our data show that deficiency in *Vlgr1* results in differences in turnover rates based on slower assembly rates of FAs.

3.3 | VLGR1 controls turnover kinetics of FAs by FRAP

We have shown that VLGR1 controls the assembly FA by our NDZ washout assays and live-cell imaging. We addressed next the effects of *Vlgr1*-deficiency on the kinetics of FA assembly by adhesions by FRAP (Figure 4). WT and *Vlgr1*-deficient astrocytes derived from Vlgr1/del7TM mouse brains were seeded onto fibronectin-coated surfaces and transfected them with Paxillin-DsRed2. Randomly selected FAs in the cell periphery of astrocytes were photobleached by the full power of laser of 560-nm excitation (Figure 4). Subsequently, fluorescence intensities in the bleached regions were determined by time-lapse imaging over a time period of 880 s (Video S3 and S4). Image analyses of the video tracks showed fast fluorescent intensity increases (FRAP) in WT astrocytes; already ~120 s after photobleaching Paxillin-DsRed2 fluorescence was recovered in FAs (Figure 4A,B, upper panels). In contrast, the recovery of Paxillin-DsRed2 was much slower in Vlgr1/del7TM astrocytes; we did not observe substantial FRAP until 240 s after photobleaching (Figure 4A,B, lower panels). FRAP signals were quantified by the online FRAP analysis tool EasyFRAP (https://easyfrap.vmnet.upatras.gr/).[23] For this, the FRAP intensities of bleached FA regions were normalized to the intensity values of background regions where noise signals were measured and to unbleached FAs where auto-fading values were measured. In Figure 4C, the quantitative analysis for the time course of Paxillin-DsRed2 fluorescence recovery is shown. The recovery of Paxillin-DsRed2 intensity was faster in WT astrocytes when compared to Vlgr1/del7TM astrocytes. In WT after 420 s approximately 50% of the Paxillin-DsRed2 fluorescence intensity of before bleaching levels were reached while in contrast, only 40% the Paxillin-DsRed2 fluorescence intensity was recovered in Vlgr1/del7TM astrocytes after that time (Figure 4C). In line with these results, we found a significantly slower average half-time ($t_{1/2}$) recovery of FRAP in Vlgr1/del7TM astrocytes with 338 s compared to WT astrocytes in which the $t_{1/2}$ was 223 s (Figure 4D). Nevertheless, our analysis by EasyFRAP revealed no significant differences in the calculated mobile fractions of Paxillin-DsRed2 between astrocytes of both WT and Vlgr1-deficent mice (Figure 4E).

Our FRAP data indicated that VLGR1 also participates in the recruitment of paxillin to FAs during their assembly.

The study was conducted in accordance with the Basic & Clinical Pharmacology & Toxicology policy for experimental and clinical studies.[27]

4 | DISCUSSION

The coordination and regulation of FA dynamics are central for cell migration under both healthy and pathological conditions.[16,24] Cell migration requires the continuous dynamic arrangement of FAs, the assembly of nascent FAs in the leading edge of cells, and disassembly in their rear.[28,29] In this regard, FAs are essential for sensing and integrating intracellular signals as well as for the reception of signals from the environment to control cell migration.[16] We previously showed that VLGR1 is part of the multiprotein complex of FAs and essential for their proper size and abundance in cells.[14,17] More importantly, our studies have also shown that VLGR1 is crucial for FA key functions, namely, in cell spreading and cell migration.[14] For this, the VLGR1 acts as a metabotropic mechanosensor sensing mechanical signals from the extracellular environment. So far, however, it had to

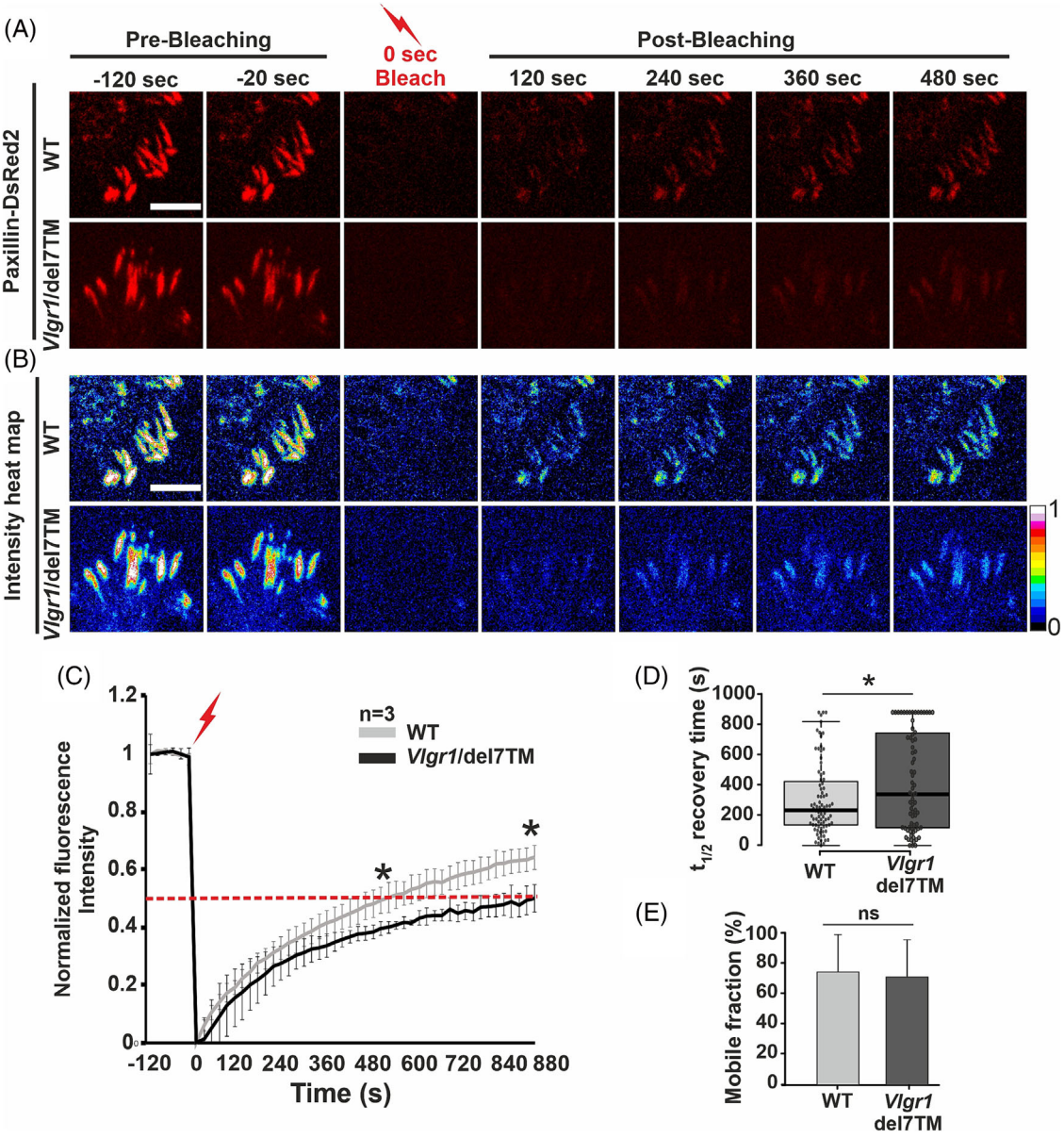

FIGURE 4 Fluorescence recovery after photo bleaching (FRAP) analysis of FAs turnover in primary astrocytes expressing Paxillin-DsRed2. (A) Representative time-lapse fluorescence images of Paxillin-DsRed2-transfected wild type (WT) and Vlgr1/del7TM primary astrocytes before and after fluorescence recovery after photobleaching (FRAP). Paxillin-DsRed2-expressed cells were imaged for 100 s before photobleaching (flash) to track basal intensity levels and bleached at 120 s. Images were acquired to record intensity recoveries for 880 s after photo bleaching. (B) Fluorescence recovery curve showing the intensity over time in the bleach ROI. From the recovery curve the immobile fraction and recovery half time can be determined. Intensity changes in individual Paxillin-DsRed2 focal adhesions during pre-bleaching and post-bleaching. (C) Normalized Paxillin-DsRed2 fluorescence intensity FRAP curves. Quantification of FRAP indicates reduction in intensity recovery in Vlgr1/del7TM astrocytes. The *red dashed line* indicates 50% of the recovery of the initial fluorescence intensity. *Asterisks* indicate significant differences in the fluorescence recovery between WT and Vlgr1/del7TM astrocytes. (D) Recovery of Paxillin-DsRed2 fluorescence after photobleaching. The recovery time after photobleaching is significantly longer Vlgr1/del7TM astrocytes (average 338 s) compared to WT astrocytes (average 233 s). (E) Mobile fractions of Paxillin-DsRed2 in WT and Vlgr1/del7TM astrocytes show no significant difference. Fluorescence recoveries normalized to pre-bleach levels and intensities of individual FA were calculated by Fiji image analysis tool and quantified by using EasyFRAP online-tool; 66–80 individual FAs were analysed in $N = 3$–7 cells of $n = 3$ experiments. Statistics: two-tailed Student's *t* test, *p % 0.05, **p % 0.01, ***p % 0.001. Scale bars: 10 μm.

remain open in which aspect of the turnover process of the dynamic macromolecular FA complexes VLGR1 participates.

In the present study, we aimed to elucidate how VLGR1 controls the FA turnover during cell migration. The turnover rate of FAs is characterized by the time

courses of their assembly and disassembly. Our data received by NDZ washout assays, live-cell imaging, and FRAP consistently provide several lines of evidence that VLGR1 regulates the turnover of FAs by participating in the assembly process of FAs. In the NDZ washout assay, FAs accumulated in response to NDZ-induced microtubule depolymerization are first rapidly degraded after NDZ washout, before FAs are reassembled.[21,25,26] Our results show that the time course of the later FA de novo assembly, but not the disassembly phase, is significantly delayed to an equal extent in the primary brain astrocytes of both *Vlgr1*-deficient mouse models studied. (Figure 2A–C; Figure S3A,B). Consistent with these findings, present live-cell imaging data acquired by monitoring the dynamics of FA turnover in living cells expressing the fluorescently tagged FA core protein paxillin[30] also demonstrated that the assembly rate but not the disassembly rate of FAs was significantly reduced in astrocytes of both *Vlgr1*-deficient mouse models (Figure 3D,E; Figure S3C,D). Present FRAP experiments also showed that the recruitment of fluorescent paxillin to FAs is slower in *Vlgr1*-deficient astrocytes (Figure 4C,D), which is in line with a reduced assembly rate of FAs as discussed above. Defects in the assembly of FAs also lead to reduced FA dynamics, which is documented by an increase of the lifetime in astrocytes of Vlgr1/DrumB mice (Figure 3F). Our data indicate that the increase of the lifespan FAs is based on a longer time span for the complete assembly of FAs as observed in Vlgr1-deficient astrocytes discussed above. All in all, these findings are consistent with the reduced migration rate in VLGR1 deficient cells that we previously found.[14]

All in all our findings on VLGR1 are consistent with the role of regulators of FA dynamics and cell migration, such as RACK1 and the phosphatidylinositol phosphate kinase type Iγ (PIPKIγ). Deficiency of VLGR1 decreases the turnover rates of the FA adaptor protein paxillin which has previously been observed for downregulation or mutations in FA regulators.[31,32]

When FAs are reassembled, integrins of disassembled FAs are recycled to the leading edge of migrating cells.[25,33,34] These integrin clusters receive signals from the extracellular matrix substrate triggering the sequential recruitment and activation of further FA components.[35–37] We have recently identified several molecules essential for the sequential assembly of FAs and related activation, such as the integrins β1, α3, α5, and α6, talin, RhoA, focal adhesion kinase (FAK), and integrin-linked kinase (ILK), as potential interacting proteins of VLGR1.[4,5,14] The absence of talin-1, one of the first FA molecules recruited to the integrin cluster, or, for example, mutations in *FAK* essential for the activation of other FA proteins, result in a delay of FA assembly but do not affect the FA disassembly rate.[25,38] This is exactly what we found in the present study for VLGR1 in *Vlgr1*-deficient cells. Taken together these data indicate that VLGR1 interplays with its interacting partners during the process of FA assembly.

The assembly of FAs as contact sites of the cell to its ECM substratum is controlled by external forces.[39] The principal membrane receptors to sense mechanical signals from the ECM are integrin dimers.[40,41] Nevertheless, there is emerging evidence that adhesion GPCRs act as mechanosensors at the cell surface, sensing mechanical forces from the extracellular environment as well.[2,42] Our recent identification of VLGR1 as a metabotropic mechanosensor in FAs,[14] in conjunction with the results found in the present study, suggests a mechanosensory role for VLGR1 in the process of FA assembly. Future studies will elucidate how the mechanosensation of integrins and VLGR1 during the assembly of FAs are coordinated.

There is growing evidence that defects in cell migration can increase susceptibility to epilepsy.[10,43] Given that the turnover of FAs is crucial for proper cell migration,[16] the altered composition rate of FAs in cells defective for VLGR1 is likely to contribute to the cellular pathophysiology in diseases caused by defects of VLGR1. VLGR1 is highly expressed in the developing CNS,[3] where the correct migration of neurons, glial cells, and their progenitors is essential.[44,45] To determine the role of VLGR1 in the turnover of FAs, we examined FA dynamics in primary brain astrocytes, which are characterized by particularly high migration properties.[46] Proper migration of astrocytes is essential for the development and maintenance of the CNS.[47] During the differentiation of the CNS, astrocytes are derived from radial glia cells in the ventricular and subventricular zone and migrate to the different layers of the brain.[47–49] In their final location, astrocytes play crucial roles in neurotransmitter clearance, synaptogenesis, and ion homeostasis and the loss of astrocyte function can lead to severe disorders of the CNS in human.[50,51] Interestingly, the loss or dysfunction of potential interacting proteins of VLGR1 in FAs, such as integrin β1, talin, or FAK can lead to astrogliosis, a hall mark in the pathogenesis of epilepsy.[52] Accordingly, VLGR1 deficiency in astrocytes may also contribute the pathophysiology underlying epilepsy, which will need to be addressed in detail in the future.

5 | CONCLUSIONS

Studying the highly mobile brain astrocytes, we validated the important role of adhesion GPCR VLGR1 in the

dynamics of FAs. Our data conclusively revealed that VLGR1 controls the kinetics of FAs by participating in the assembly of FAs, thereby the migration of the cells. For this, VLGR1 may act as a metabotropic mechanosensor sensing in parallel with integrins mechanical signals from the environment. Our findings not only elucidate the molecular and cellular function of VLGR1 in healthy brain astrocytes but also provide novel insights into the pathomechanisms of VLGR1-associated epilepsy.

ACKNOWLEDGEMENTS

We thank Drs. Rudolf E. Leube and Rick Hortwitz for kindly providing the Paxillin-DsRed2 plasmid, Dr. Kerstin Nagel-Wolfrum for fruitful discussions on the manuscript, and Susanne Wilhelm for language editing. Open Access funding enabled and organized by Projekt DEAL.

CONFLICT OF INTEREST STATEMENT

The authors declare no conflict of interest.

INSTITUTIONAL REVIEW BOARD STATEMENT

The use of mice in research was approved by the German regulation authority for the use of animals in research, the district administration Mainz-Bingen, 8341a/177-5865-§11 ZVTE, 30.04.2014.

ORCID

Baran E. Güler https://orcid.org/0000-0001-7967-9041
Uwe Wolfrum https://orcid.org/0000-0002-4756-5872

REFERENCES

1. Hamann J, Aust G, Araç D, et al. International union of basic and clinical pharmacology. XCIV. Adhesion G protein-coupled receptors. *Pharmacol Rev*. 2015;67(2):338-367. doi:10.1124/pr.114.009647
2. Lala T, Hall RA. Adhesion G protein-coupled receptors: structure, signaling, physiology, and pathophysiology. *Physiol Rev*. 2022;102(4):1587-1624. doi:10.1152/physrev.00027.2021
3. McMillan DR, White PC. Studies on the very large G protein-coupled receptor: from initial discovery to determining its role in sensorineural deafness in higher animals. *Adv Exp Med Biol*. 2010;706:76-86. doi:10.1007/978-1-4419-7913-1_6
4. Knapp B, Roedig J, Boldt K, et al. Affinity proteomics identifies novel functional modules related to adhesion GPCRs. *Ann N Y Acad Sci*. 2019;1456(1):144-167. doi:10.1111/nyas.14220
5. Knapp B, Roedig J, Roedig H, et al. Affinity proteomics identifies interaction partners and defines novel insights into the function of the adhesion GPCR VLGR1/ADGRV1. *Molecules*. 2022;27(10):3108. doi:10.3390/molecules27103108
6. Liebscher I, Schöneberg T. Tethered agonism: a common activation mechanism of adhesion GPCRs. In: *Adhesion G Protein-coupled Receptors. Handbook of Experimental Pharmacology*. Springer; 2016:111-125. doi:10.1007/978-3-319-41523-9_6
7. Liebscher I, Schöneberg T, Thor D. Stachel-mediated activation of adhesion G protein-coupled receptors: insights from cryo-EM studies. *Signal Transduct Target Ther*. 2022;7(1):227. doi:10.1038/s41392-022-01083-y
8. Fuster-García C, García-Bohórquez B, Rodríguez-Muñoz A, et al. Usher syndrome: genetics of a human ciliopathy. *Int J Mol Sci*. 2021;22(13):1-25. doi:10.3390/ijms22136723
9. Wolfrum U. Protein networks related to the Usher syndrome gain insights in the molecular basis of the disease. In: Ahuja S, ed. *Usher Syndrome: Pathogenesis, Diagnosis and Therapy*. Nova Science Publishers, Inc.; 2011:51-73.
10. Zhou P, Meng H, Liang X, et al. ADGRV1 variants in febrile seizures/epilepsy with antecedent febrile seizures and their associations with audio-visual abnormalities. *Front Mol Neurosci*. 2022;15:864074. doi:10.3389/fnmol.2022.864074
11. Dahawi M, Elmagzoub MS, A. Ahmed E, et al. Involvement of ADGRV1 gene in familial forms of genetic generalized epilepsy. *Front Neurol*. 2021;12:738272. doi:10.3389/fneur.2021.738272
12. Michel V, Goodyear RJ, Weil D, et al. Cadherin 23 is a component of the transient lateral links in the developing hair bundles of cochlear sensory cells. *Dev Biol*. 2005;280(2):281-294. doi:10.1016/j.ydbio.2005.01.014
13. Maerker T, van Wijk E, Overlack N, et al. A novel Usher protein network at the periciliary reloading point between molecular transport machineries in vertebrate photoreceptor cells. *Hum Mol Genet*. 2008;17(1):71-86. doi:10.1093/hmg/ddm285
14. Kusuluri DK, Güler BE, Knapp B, et al. Adhesion G protein-coupled receptor VLGR1/ADGRV1 regulates cell spreading and migration by mechanosensing at focal adhesions. *iScience*. 2021;24(4):102283. doi:10.1016/j.isci.2021.102283
15. Geiger B, Spatz JP, Bershadsky AD. Environmental sensing through focal adhesions. *Nat Rev Mol Cell Biol*. 2009;10(1):21-33. doi:10.1038/nrm2593
16. Mishra YG, Manavathi B. Focal adhesion dynamics in cellular function and disease. *Cell Signal*. 2021;85(May):110046. doi:10.1016/j.cellsig.2021.110046
17. Güler BE, Krzysko J, Wolfrum U. Isolation and culturing of primary mouse astrocytes for the analysis of focal adhesion dynamics. *STAR Protoc*. 2021;2(4):100954. doi:10.1016/j.xpro.2021.100954
18. McMillan DR, White PC. Loss of the transmembrane and cytoplasmic domains of the very large G-protein-coupled receptor-1 (VLGR1 or Mass1) causes audiogenic seizures in mice. *Mol Cell Neurosci*. 2004;26(2):322-329. doi:10.1016/j.mcn.2004.02.005
19. Potter PK, Bowl MR, Jeyarajan P, et al. Novel gene function revealed by mouse mutagenesis screens for models of age-related disease. *Nat Commun*. 2016;7(August):1-13. doi:10.1038/ncomms12444
20. Pora A, Yoon S, Windoffer R, Leube RE. Hemidesmosomes and focal adhesions treadmill as separate but linked entities during keratinocyte migration. *J Invest Dermatol*. 2019;139(9):1876-1888. doi:10.1016/j.jid.2019.03.1139
21. Ezratty EJ, Partridge MA, Gundersen GG. Microtubule-induced focal adhesion disassembly is mediated by dynamin

and focal adhesion kinase. *Nat Cell Biol*. 2005;7(6):581-590. doi:10.1038/ncb1262
22. Berginski ME, Vitriol EA, Hahn KM, Gomez SM. High-resolution quantification of focal adhesion spatiotemporal dynamics in living cells. *PLoS ONE*. 2011;6(7):e22025. doi:10.1371/journal.pone.0022025
23. Koulouras G, Panagopoulos A, Rapsomaniki MA, Giakoumakis NN, Taraviras S, Lygerou Z. EasyFRAP-web: a web-based tool for the analysis of fluorescence recovery after photobleaching data. *Nucleic Acids Res*. 2018;46(W1):W467-W472. doi:10.1093/nar/gky508
24. Gardel ML, Schneider IC, Aratyn-Schaus Y, Waterman CM. Mechanical integration of actin and adhesion dynamics in cell migration. *Annu Rev Cell Dev Biol*. 2010;26(1):315-333. doi:10.1146/annurev.cellbio.011209.122036
25. Nader GPF, Ezratty EJ, Gundersen GG. FAK, talin and PIPKIγ regulate endocytosed integrin activation to polarize focal adhesion assembly. *Nat Cell Biol*. 2016;18(5):491-503. doi:10.1038/ncb3333
26. Assar EA, Tumbarello DA. Loss of the essential autophagy regulators FIP200 or Atg5 leads to distinct effects on focal adhesion composition and organization. *Front Cell Dev Biol*. 2020;8(August):1-15. doi:10.3389/fcell.2020.00733
27. Tveden-Nyborg P, Bergmann TK, Jessen N, Simonsen U, Lykkesfeldt J. BCPT policy for experimental and clinical studies. *Basic Clin Pharmacol Toxicol*. 2021;128(1):4-8. doi:10.1111/bcpt.13492
28. Ridley AJ, Schwartz MA, Burridge K, et al. Cell migration: integrating signals from front to back. *Science (80-)*. 2003;302(5651):1704-1709. doi:10.1126/science.1092053
29. Parsons JT, Horwitz AR, Schwartz MA. Cell adhesion: integrating cytoskeletal dynamics and cellular tension. *Nat Rev Mol Cell Biol*. 2010;11(9):633-643. doi:10.1038/nrm2957
30. Stehbens SJ, Wittmann T. Analysis of focal adhesion turnover: a quantitative live-cell imaging example. In: *Methods in Cell Biology*. Vol.123. Academic Press; 2014:335-346. doi:10.1016/b978-0-12-420138-5.00018-5
31. Doan AT, Huttenlocher A. RACK1 regulates Src activity and modulates paxillin dynamics during cell migration. *Exp Cell Res*. 2007;313(12):2667-2679. doi:10.1016/j.yexcr.2007.05.013
32. Wu Z, Li X, Sunkara M, Spearman H, Morris AJ, Huang C. Pipkiγ regulates focal adhesion dynamics and colon cancer cell invasion. *PLoS ONE*. 2011;6(9):e24775. doi:10.1371/journal.pone.0024775
33. Caswell P, Norman J. Endocytic transport of integrins during cell migration and invasion. *Trends Cell Biol*. 2008;18(6):257-263. doi:10.1016/j.tcb.2008.03.004
34. Chao W-T, Kunz J. Focal adhesion disassembly requires clathrin-dependent endocytosis of integrins. *FEBS Lett*. 2009;583(8):1337-1343. doi:10.1016/j.febslet.2009.03.037
35. Roca-Cusachs P, Gauthier NC, Del Rio A, Sheetz MP. Clustering of α5β1 integrins determines adhesion strength whereas αvβ3 and talin enable mechanotransduction. *Proc Natl Acad Sci U S A*. 2009;106(38):16245-16250. doi:10.1073/pnas.0902818106
36. Byron A, Humphries JD, Craig SE, Knight D, Humphries MJ. Proteomic analysis of α4β1 integrin adhesion complexes reveals α-subunit-dependent protein recruitment. *Proteomics*. 2012;12(13):2107-2114. doi:10.1002/pmic.201100487
37. Baade T, Paone C, Baldrich A, Hauck CR. Clustering of integrin β cytoplasmic domains triggers nascent adhesion formation and reveals a protozoan origin of the integrin-talin interaction. *Sci Rep*. 2019;9(1):5728. doi:10.1038/s41598-019-42002-6
38. Zhu L, Plow EF, Qin J. Initiation of focal adhesion assembly by talin and kindlin: a dynamic view. *Protein Sci*. 2021;30(3):531-542. doi:10.1002/pro.4014
39. Riveline D, Zamir E, Balaban NQ, et al. Focal contacts as mechanosensors: externally applied local mechanical force induces growth of focal contacts by an mDia1-dependent and ROCK-independent mechanism. *J Cell Biol*. 2001;153(6):1175-1185. doi:10.1083/jcb.153.6.1175
40. Elosegui-Artola A, Oria R, Chen Y, et al. Mechanical regulation of a molecular clutch defines force transmission and transduction in response to matrix rigidity. *Nat Cell Biol*. 2016;18(5):540-548. doi:10.1038/ncb3336
41. Bachmann M, Schäfer M, Mykuliak VV, et al. Induction of ligand promiscuity of αVβ3 integrin by mechanical force. *J Cell Sci*. 2020;133(9):jcs242404. doi:10.1242/jcs.242404
42. Langenhan T. Adhesion G protein–coupled receptors—candidate metabotropic mechanosensors and novel drug targets. *Basic Clin Pharmacol Toxicol*. 2020;126(S6):5-16. doi:10.1111/bcpt.13223
43. Qin R, Cao S, Lyu T, Qi C, Zhang W, Wang Y. CDYL deficiency disrupts neuronal migration and increases susceptibility to epilepsy. *Cell Rep*. 2017;18(2):380-390. doi:10.1016/j.celrep.2016.12.043
44. Buchsbaum IY, Cappello S. Neuronal migration in the CNS during development and disease: insights from in vivo and in vitro models. *Development*. 2019;146(1):dev163766. doi:10.1242/dev.163766
45. Lago-Baldaia I, Fernandes VM, Ackerman SD. More than mortar: glia as architects of nervous system development and disease. *Front Cell Dev Biol*. 2020;8:611269. doi:10.3389/fcell.2020.611269
46. Zhan JS, Gao K, Chai RC, et al. Astrocytes in migration. *Neurochem Res*. 2017;42(1):272-282. doi:10.1007/s11064-016-2089-4
47. Siracusa R, Fusco R, Cuzzocrea S. Astrocytes: role and functions in brain pathologies. *Front Pharmacol*. 2019;10:1114. doi:10.3389/fphar.2019.01114
48. Tabata H. Diverse subtypes of astrocytes and their development during corticogenesis. *Front Neurosci*. 2015;9:114. doi:10.3389/fnins.2015.00114
49. Platel JC, Bordey A. The multifaceted subventricular zone astrocyte: from a metabolic and pro-neurogenic role to acting as a neural stem cell. *Neuroscience*. 2016;323:20-28. doi:10.1016/j.neuroscience.2015.10.053
50. Iram T, Ramirez-Ortiz Z, Byrne MH, et al. Megf10 is a receptor for C1Q that mediates clearance of apoptotic cells by astrocytes. *J Neurosci*. 2016;36(19):5185-5192. doi:10.1523/JNEUROSCI.3850-15.2016
51. Allen NJ, Eroglu C. Cell biology of astrocyte-synapse interactions. *Neuron*. 2017;96(3):697-708. doi:10.1016/j.neuron.2017.09.056

52. Robel S, Mori T, Zoubaa S, et al. Conditional deletion of β1-integrin in astroglia causes partial reactive gliosis. *Glia*. 2009;57(15):1630-1647. doi:10.1002/glia.20876

SUPPORTING INFORMATION

Additional supporting information can be found online in the Supporting Information section at the end of this article.

How to cite this article: Güler BE, Linnert J, Wolfrum U. Monitoring paxillin in astrocytes reveals the significance of the adhesion G protein coupled receptor VLGR1/ADGRV1 for focal adhesion assembly. *Basic Clin Pharmacol Toxicol*. 2023;1-12. doi:10.1111/bcpt.13860